Submission Date: 2023-07-25
Accepted Date: 2024-01-17
Accepted Manuscript online: 2024-04-04

Journal of Neurological Surgery Part A: Central European Neurosurgery

The value of SINO robot combined with Angio Render technology-assisted stereo-electroencephalography electrode implantation for the treatment of drug-resistant epilepsy

Yihai Dai, Rifeng Jiang, Jingyi Zhang, Zhe Qian, Zhen Chen, Songsheng Shi, Shiwei Song.

Affiliations below.

DOI: 10.1055/a-2299-7781

Please cite this article as: Dai Y, Jiang R, Zhang J et al. The value of SINO robot combined with Angio Render technology-assisted stereo-electroencephalography electrode implantation for the treatment of drug-resistant epilepsy. Journal of Neurological Surgery Part A: Central European Neurosurgery 2024. doi: 10.1055/a-2299-7781

Conflict of Interest: The authors declare that they have no conflict of interest.

This study was supported by Fujian Provincial Natural Science Foundation Program, 2021J01788, The Startup Fund for scientific research, Fujian Medical University, 2021QH1048, Joint Funds for the Innovation of Science and Technology, Fujian province, 2018Y9059

Abstract:

Abstract
Background and objective: Stereo-electroencephalography (SEEG) electrodes are implanted using a variety of stereotactic technologies to treat refractory epilepsy. The value of SINO-robot for SEEG electrode implantation is rarely reported. The aim of the current study was to assess the value of SINO-robot in conjunction with Angio Render technology, in SEEG electrode implantation. We also assess its efficacy by examining factors such as localization error, operation time, and complications.
Methods: Between June 2018 and October 2020, we retrospectively reviewed 58 patients who underwent SEEG implantation to resect or ablate their epileptogenic zone (EZ) while minimizing the risk of hemorrhage. SINO-robot combined with Angio Render technology-assisted SEEG electrode implantation was used to visualize each patient' blood vessel in a 3D plane. The 3D view functionality was used to increase the safety and accuracy of the implantation, and reducing the risk of hemorrhage by avoiding said blood vessel.
Results: In this study, 634 SEEG electrodes were implanted in 58 patients. The mean 10.92(range 5- 18) leads per patient. The mean entry point localization error (EPLE) was 0.94 ± 0.23 mm (range: 0.39– 1.63 mm), and the mean target point localization error (TPLE) was 1.49 ± 0.37 mm (range: 0.80–2.78 mm). The mean operating time per lead (MOTPL) was 6. 18 ± 1.80 min (range: 3.02– 14.61 min). And the mean depth of electrodes was 56.96± 3.62 mm (range:27.23–124.85 mm). At a follow-up of at least one year, totally 81.57% (47/58) of patients achieved an Engel class I of seizure freedom. There were 2 patients with asymptomatic brain hematomas following SEEG placement, and no late complications or mortality in this cohort.
Conclusions: SINO-robot in conjunction with Angio Render technology assist, in SEEG electrode implantation is safe and accurate in mitigating the risk of intracranial hemorrhage in patients suffering from drug-resistant epilepsy.

Corresponding Author:
Shiwei Song, Fujian Medical University Union Hospital, Department of Neurosurgery,, Fuzhou, China, shiweisong@fjmu.edu.cn

Affiliations:
Yihai Dai, Fujian Medical University Union Hospital, Neurosurgery, fuzhou, China
Rifeng Jiang, Fujian Medical University Union Hospital, Department of Imaging, Fuzhou, China
Jingyi Zhang, Fujian Medical University Union Hospital, Department of Neurosurgery, Fuzhou, China
[...]
Shiwei Song, Fujian Medical University Union Hospital, Department of Neurosurgery,, Fuzhou, China

Thieme

The value of SINO robot combined with Angio Render technology-assisted stereo-electroencephalography electrode implantation for the treatment of drug-resistant epilepsy

Introduction

Epilepsy is a medically significant condition that exhibits a considerable prevalence across various age groups. Despite notable advancements in the field of antiepileptic drugs, a substantial proportion of individuals, exceeding 30%, continue to experience drug-resistant epilepsy.[1]. Epilepsy surgery is recognized as a highly successful treatment for drug-resistant epilepsy. Patients who have had surgery for drug-resistant epilepsy have increased dramatically during the past 20 years[2]. Accurate pre-operative localization of the epileptogenic zone (EZ) and understanding of the epileptic network are essential for epilepsy surgery. Stereo-electroencephalography (SEEG) is an accurate, safe, and effective procedure for localizing EZ in drug-resistant epilepsy patients[3] SEEG can be helpful for the 3-dimensional (3D) definition of the EZ, and this methodology is gaining popularity worldwide[4]·Precise surgical planning and reliable stereotactic technique ensure safe implantation of SEEG electrodes[3]. Many neurosurgical centers have applied multimodal image fusion technology in epilepsy surgery, especially the cerebrovascular reconstruction technology. Several stereotactic technologies[5], such as classic frame-based[6], frameless navigation[7], and robotic guidance approaches[8], are now used to implant SEEG electrodes in different neurosurgical centers. Although there are many phantom studies on stereotactic systems and devices, application accuracy in actual surgery is affected by a variety of circumstances. The evaluation of in vivo accuracy in deep brain stimulation procedures, biopsies, catheter insertion, guided craniotomies, and depth electrodes has been the subject of several papers[8-10]. They reported that the frameless ROSA robot-assisted SEEG implantation for drug-resistant epilepsy patients was safe and effective [11-14].

As a newly marketed machine, SINO-robot (Sinovation® Medical, Beijing, China) is specifically designed as a stereotactic device, it consists of a robot arm with a high-precision six-axis force sensor and a mobile case as a base unit. The device is equipped with a high-precision pressure sensor and guided by a custom algorithm. It can monitor its force feedback in real time, stopping its movement when encountering obstacles, such as a doctor or patient.

The SinoPlan system, which specializes in neurosurgical operation planning, is tailor-made for clinical usage. It relies on Angio Render technology, developed for cortical vessel imaging and visualization, to minimize intracranial hemorrhage risk during depth electrode insertion[15].The Angio Render Technology can implement cortical vessel imaging and visualization based on Computed Tomography Angiography (CTA) data, Digital Subtraction Angiography (DSA)data, or Magnetic Resonance Angiography (MRA)data /Magnetic Resonance Venography (MRV） data. The SinoPlan system realizes optimal co-registered 3D views of the sulcal anatomy and vasculature of the brain, a critical ability to plan SEEG trajectories. SEEG trajectories and intracranial vessels can be displayed in three-dimensional space directly in the SinoPlan system. The imaging system of SINO-robot was established on SinoPlan system.

Few studies reported the application of SINO robot combined with Angio Render technology-assisted SEEG in electrode implantation. The objective of the current study was to assess the value of SINO-robot in conjunction with Angio Render technology, in SEEG electrode implantation. We also assess its efficacy by examining factors such as localization error, operation time, and complications.

Subjects

Between June 2018 and October 2020, we reviewed 58 consecutive patients who met the International League Against Epilepsy's criterion of drug-resistant epilepsy [16] All the patients underwent SINO robot-guided SEEG electrode implantation, and were divided into those who underwent either epileptic lesion removal surgery and those who underwent radiofrequency thermocoagulation(RFTC). This study was conducted under the ethical standards of the Declaration of Helsinki. It was approved by the Ethics Committee Board of Fujian Medical University Union Hospital, and informed consent was obtained from all participants.

MRI acquisition

All images were acquired using a 3T MR scanner (MAGNETOM Prisma, Siemens Healthcare, Erlangen, Germany). The high-resolution structural MRI protocol included sagittal T1-weighted magnetization-prepared rapid acquisition with gradient echo image (T1-MPRAGE), axial T2-weighted (T2W) fast spin-echo (FSE) images, and axial fluid-attenuated inversion recovery (FLAIR) T2W images.

CE-MRAV was performed in the axial plane immediately after 3D-TOF-MRA. Contrast material (Gadobutrol - 0.1 mmol/kg) was injected via the ante-cubital vein at a rate of 2.5 ml/s followed by a saline (0.9%) bolus of 20 ml at 2.5 ml/s. The 3D volume was acquired with the following imaging parameters: TR=3.70ms, TE=1.32ms, slice thickness=1.2mm, pixel bandwidth=390 Hz/pixel , FA=22°, field of view=240×195 mm2; voxel size =0.6×0.6×1.2 mm3. Parallel image acquisition using GRAPPA (Generalized Autocalibrating Partially Parallel Acquisition) algorithm was applied with an acceleration factor of 3.

Trajectory Planning

Within the SINO platform, medical professionals engage in the process of reconstructing various components of the patient's brain, including the tissue structure, skull, blood vessels, brain conduction bundles, and other relevant anatomical aspects. These components are subsequently integrated and fused together. The cerebral cortex was reconstructed using a thin-layer T2flair sequence, while the cerebral vasculature was reconstructed using a CE-MRAV (Contrast-Enhanced Magnetic Resonance Angio-Venogram) sequence. The skull layer was imaged using a thin-scan CT sequence, and the scalp was visualized using a TI3D sequence. Initially, the SINO platform was employed to perform co-registration of thin-slice head CT scans with a thickness of 1 mm to head MRI scans also with a thickness of 1 mm. Subsequently, the reconstructed blood vessels were generated using contrast-enhanced magnetic resonance angiography (CE-MRAV) data. To assure surgical safety, it is imperative to visualize all vessels with a diameter higher than 1 mm. It is worth mentioning that the unique Angio Render vascular 3D visualization technology of the SINO platform can fully display the intracranial vascular structure[15].Therefore, it allows surgeons to directly plan electrode trajectories from a three-dimensional view, effectively avoiding the main blood vessels (Fig. 1). The minimum distance of trajectory planning from vessels is 2mm. Neurosurgeons can devise a SEEG implantation strategy through the utilization of three-dimensional image reconstruction techniques.

The number and position of electrodes implanted were determined by prior working hypotheses regarding the localization of the EZs based on semiology, scalp EEG data, and the results of other non-invasive investigations (MRI, PET). The aims of SEEG planning are as follows:1) to identify the epileptogenic zone (EZ), 2) to investigate its association with functional regions, and 3) to assess the possibility of surgical excision[17]. The precision of the implant, electrodes is enhanced by Orthogonal trajectories, while oblique trajectories can help sample the cortical convexity[17].The SINO-robotic guiding platform may realize oblique electrode trajectories if necessary and does not require totally orthogonal electrode trajectories. The process of SEEG implantation typically entails the placement of electrodes in a single hemisphere, although there are infrequent instances where both hemispheres are involved. Bilateral monitoring was also convenient if there was any question about onset laterality in some patients due to negative lateralizing information after ictal scalp EEG and functional imaging, especially the bitemporal lobe epilepsy[18]. Avascular trajectories of the electrodes were determined by three-dimensional T1-weighted brain MRI, and magnetic resonance angiography was computed with stereotactic software (Sinovation Medical, Beijing, China) during preoperative planning. The software was used to direct the robotic arm connected to a Mayfield or Dora 3-pin frame during the implantation of the electrodes (0.8 mm diameter, 8–16 contacts, 2mm length, 1.5mm spacing). To calculate the electrode length accurately and conveniently, the entry point (EP) was set on the scalp (Fig. 2).

Surgical procedure

Preoperative five or six bone fiducials (Sinovation® Medical, Beijing, China) were placed around the surgical field under local anesthesia to improve the accuracy of localization[19]. Then a thin-slice (1 mm) head CT scan was performed and co-registered with the planning MRI images.

The patients were then positioned either supine, laterally, or prone while under general anesthesia. Patients were then placed in the Mayfield clamp with their heads firmly secured to the operating table (patients younger than 3 years old had their skulls fixed with pediatric head nails, and those more than 10 years old had adult head nails). The SINO platform base was attached to the headframe. The patient underwent registration to the CT planning image by utilizing a robotic arm for bone fiducial recognition. (Fig.3 a). After strict sterile preparation of the surgical area, the operation begins. The robotic arm alternately moving to each planned trajectory.

The high-precision pressure sensor on the robotic arm played an important role.

When the surgeon stepped on a foot-operated safety switch, they could simultaneously drag the end of the robotic arm. The high-precision pressure sensor could sense the force on the robotic arm and control it to move with the operator's hand. Then, the end of the robotic arm could only move in the previously determined direction of the electrode trajectories. With this technology, the distance between the end of the robotic arm and the patient's head could be adjusted, greatly facilitating the subsequent operation.

Once the entry point was identified, a 2 mm drill bit was utilized to generate twist drill holes for direct access to the skull, under the control of a robotic arm (Fig 3b). The bone debris within the cranial aperture was irrigated, followed by the insertion of a sharp coagulation electrode with a diameter of 2 mm to penetrate the dura mater and halt the hemorrhaging. Subsequently, the guide anchor bolts were securely fastened into the designated aperture (see Fig 3c). The length of the target trajectory was measured by using a stylet, which punctured the brain to provide an opening for the electrode route (see Fig 3d). The SEEG electrodes were identified as desired length using rubber rings, as depicted in Fig 3e. The SEEG electrodes were placed into the designated hole with the guidance of an anchor bolt to achieve the desired length. Subsequently, the electrodes were fastened using polyurethane bolt caps, as depicted in Fig 3f. Subsequently, the robotic arm proceeded to the subsequent target. Following the insertion of all electrodes, Vaseline gauze was applied around each bolt and subsequently covered with sterile gauze. A postoperative CT scan was performed and co-registered with the preoperative MRI to pinpoint the location of each contact in the software workstation (Sinovation) and to ensure the absence of postoperative bleeding and the accuracy of the electrode implantation.

SEEG Recording

Extra operative SEEG recordings were performed in chronic conditions (1 week to 1 month) with reduced medication to capture spontaneous habitual seizures using a video-EEG system (Neuvo Amplifier, Neuroscan Compumedics, Australia) that allowed simultaneous recording of up to 256 contacts at a sampling rate of 10000 Hz (bandpass filter of 0–2500 Hz). Depth EEG activity was observed between contiguous contacts at various levels along the axis of each electrode, and visual analysis was performed on SEEG traces to determine interictal and ictal patterns. Prior to the clinical onset of the seizure, the area displaying the initial distinct SEEG change was visually designated as the seizure-onset zone (SOZ). When SEEG ictal onsets exhibited low-voltage fast activity in the beta and gamma bands, or recruiting and periodic rapid discharge of spikes, they were deemed significant. When interictal epileptiform discharges (IEDs) comprised spikes, poly spikes, spike-and-wave complexes, or poly spike and wave complexes, they were deemed significant. Electrical stimulations were carried out after the patients experienced 2-3 habitual seizures or auras. Electrically elicited seizures (EES) were deemed significant when they demonstrated clinical similarity to spontaneously recorded seizures.

RF-TC And Resection

In all patients, the strategy of surgical resection and SEEG-guided radiofrequency coagulation was discussed during a patient management conference based on multimodal data, including MRI, positron emission tomography, video EEG, and SEEG, after the EZ was determined[20,21].

The SINO platform still plays a very important role in determining RFTC contacts, which can support the three-dimensional measurement of the distance between contacts and intracranial vascular. It was believed that the range of RF-TC could be largest at appropriate parameter, and the resulting lesions were reported to be 5–7 mm in diameter[22]. Therefore, we advocate that the distance between contacts and intracranial vascular more than 4mm is a safe distance for RF-TC.

SEEG-guided RFTC was performed without anesthesia using a radiofrequency generator system (Model No. R2000B-M1, BNS, Beijing, China) at the conclusion of the recording period and prior to removing the electrodes, allowing for clinical monitoring of the patient throughout the procedure. In 40 seconds, a maximal output of 7.5 W from the generator produced lesions between two adjacent contacts of the selected electrodes. In patients with a history of frequent seizures prior to RFTC, SEEG surveillance was sometimes extended for a few days following thermocoagulation. A second RFTC procedure would be performed if seizures persisted following the initial SEEG-guided RFTC procedure. The electrodes were removed under anesthesia one to two days after the completion of the final RFTC procedure, and the patients were subsequently discharged.

Following a precise delineation of the boundary, a neuro-navigation craniotomy procedure could be conducted, since the SINO platform continues to hold significant relevance in the field of craniotomy. Prior to the surgical procedure, it is imperative to establish a comprehensive understanding of the vascular architecture near the anatomical boundary, employing a three-dimensional approach. It is arguable that prioritizing the protection of cerebral blood arteries could yield greater advantages. Furthermore, in cases where neuronavigational mistakes were induced by brain shift during surgical procedures, the three-dimensional vascular structure might be employed to identify the precise location of the surgically excised boundary.

Data Analysis and outcome

The study retrospectively examined and reported on many factors, including demographic data, the number of electrodes, surgery duration and accuracy. Additionally, information on seizure outcomes and complications associated with the procedure were also gathered. The time from locating the first trajectory to securing the last electrode was defined as operating time (OPT). The patients' outcome was quantified at least 1 year after the procedure by an epileptologist based on the Engel outcome scale The preoperative MRI was co-registered with the post-operative CT scans in order to visualize the actual electrode position and evaluate the positioning accuracy. The entry point localization error (EPLE) or the target point localization error (TPLE) was defined as the Euclidean distance between the planned entry point or target point coordinates and the coordinates of the post-implantation electrode entry point or target point. The actual location coordinates (Xa, Ya, Za) and planned location coordinates (Xb, Yb, Zb) were recorded by the SINO platform workstation. The localization errors between entry and target point were calculated for each electrode (Fig. 4), applying the following formula[23] (Equation1):

$$\text{Placement error} = \sqrt{(Xa - Xb)^2 + (Ya - Yb)^2 + (Za - Zb)^2}$$

Equation1. The localization errors between entry and target point.

The depth of electrodes was defined as the Euclidean distance between post-implantation entry point to target point. And it has the same formula as Equation1.

In the Results section, the overall placement error is shown as the mean ± standard deviation (SD).

Results

Within two years, there were 58 patients with a mean age of 18. 10±12.97 years (range:4–45 years; 32 males, 26 females). Totally,634 SEEG electrodes were implanted and the aggregate of SEEG electrodes was 10.92 (range: 5– 18) electrodes per patient. Six patients had bilateral electrode implantation. The mean operating time per lead (MOTPL) was 6. 18±1.80 min (range: 3.02– 14.61 min). The mean entry point localization error (EPLE) was 0.94 ± 0.23 mm (range: 0.39– 1.63 mm,), and the mean target point localization error (TPLE) was 1.49 ± 0.37 mm (range: 0.80–2.78 mm). And the mean depth of electrodes was 56.96± 3.62 mm (range:27.23–124.85 mm). And more details are summarized in Table2.

Seventeen patients underwent surgical resection (9 anterior temporal lobectomy; 5 frontal epileptic focal resection; 3 parietal epileptics focal resection). The remaining 41 patients underwent SEEG-guided RF-TC (including 6 hypothalamic hamartomas).

Complications

No notable complications were observed in this study. However, asymptomatic intracranial hemorrhage was detected on postoperative CT in two cases following implantation (three implanted electrodes), in eight cases following SEEG-guided RF-TC, and in two cases following surgical resection. No instances of infection were seen following in this study.

Epilepsy Outcomes

In the present investigation, all participants underwent follow-up assessments for a minimum duration of one year. In the RF-TC group, a total of 41 patients were included in the analysis. Among these patients, 33 out of 41 (80.48%) achieved seizure freedom and were classified as Engel class I. Additionally, 6 out of 41 patients (14.63%) were classified as Engel class II, indicating a partial reduction in seizures. Lastly, 2 out of 41 patients (4.89%) were classified as Engel class III, indicating a lack of improvement in seizure control. In the resection group, a total of 82.35% (14 out of 17) of patients achieved seizure freedom according to the Engel class I classification. The remaining 17.65% (3 out of 17) of patients fell into the Engel class II category. (Table3).

Discussion

The aim of the current study was to assess the value of SINO-robot in conjunction with Angio Render technology, in SEEG electrode implantation. The primary focus was on assessing the safety and accuracy of this approach in mitigating the risk of intracranial hemorrhage in patients suffering from drug-resistant epilepsy. We also assess the efficacy of SINO-robot assisted stereo electroencephalography electrode implantation by examining factors such as localization error, operation time, and complications.

Vakharia et al. published a meta-analysis and systematic review about the accuracy of SEEG electrode placement for [5] .Their study showed that ROSA robotic assisted stereo-electroencephalography had a mean EPLE of 1. 17 mm (95% CI: 0.80– 1.53 mm) and a TPLE of 1.71 mm (95% CI: 1.66– 1.75 mm). In our study, the SINO-robotic trajectory guidance system was at least as accurate as other systems. The accuracy of each operation was consistent because the SINO-robotic trajectory guidance systems clearly indicated the entry point position and electrode length. The neurosurgeon followed the instructions to ensure the accuracy and safety of the operation. The previously reported studies about stereotactic robots of this property are summarized in Table 1.

As for the mean operating time per electrode, different units may use different devices, which we believe is related to the convenience of the devices as well as the proficiency and tacit cooperation of the operators. A systematic review and meta-analysis indicate that the mean operating time per electrode in robot-assisted group is significantly less than that in the traditional hand-guided group [24]. On the other hand, another systematic review and meta-analysis about robotic-assisted stereo electroencephalography description the mean operating time per electrode of Sinovation(9.9min) is shorter than that in ROSA (11.45min)[25]. Martínez et al reported the results of 101 robot-assisted SEEG procedures[26]. In total, with the help of the ROSA-robotic trajectory guidance system,1245 depth electrodes were implanted, with the mean operating time per electrode of 10.4 min[26]. Spyrantis et al. performed five robot-assisted SEEG procedures with the ROSA robotic trajectory guidance system; 40 SEEG electrodes were implanted in total; the mean operating time per lead was 9.38 min. In our series of cases, the mean operating time per lead was 6.18 ± 1.80 min, a markedly reduced time compared to previous reports; we attribute this result to the SINO robot’s excellent performance, the proficiency and tacit cooperation of the operators.

In Wang et study[15]□they compared PC-MRA images with intraoperative photographs for the first time to evaluate the effectiveness of cortical vascular imaging, and the results showed good agreement. Although just a small number of lost vessels (17of 93, 18.3%) were found, they were all buried in the sulci. A clearer sulci visualization could greatly aid surgical planning since the sulci could be rendered darker in the cortex volume rendering according to their depth information. This finding strongly implies that the cortex vision accuracy is crucial for enhancing the cortical arteries' structural integrity and preventing ICH to the greatest extent. The sulcal anatomy and vasculature may be seen in the best co-registered 3D views thanks to the SINO-Angio robot's Render technology. It offers a secure and reliable approach for implanting SEEG electrodes to define the epileptogenic zone in patients with drug-resistant epilepsy.

Cardinale et al. published a meta-analysis and systematic review about the morbidity and mortality of SEEG electrodes placement[27] [14]. This study shows that 35 major complications (including four fatalities) were reported in approximately 4000 patients implanted with approximately 33,000 electrodes. In the four fatal cases, three intraoperative large intracranial hemorrhages were described: one in Lyon[28] , one in Rouen[29], and one at CCF(carotid cavernous fistula) [30]. Other major immediate complications after electrode implantation included 14 cases of non-fatal intracranial hemorrhage. Mullin et al. published another systematic review of the morbidity and mortality of intracranial SEEG electrode placement[31]. The first two most common complications reported were hemorrhagic (pooled prevalence:1.0%,95% CI 0.6–1.4%) and infectious (pooled prevalence: 0.8%, 95% CI 0.3– 1.2%). Therefore, reducing the incidence of intracranial hemorrhage would positively affect the morbidity and mortality of intracranial SEEG implantation.

The risk of cerebral hemorrhage during stereotactic neurosurgery procedures can cause severe morbidity and mortality. Planning stereotactic procedures to avoid conflicts with the cerebral vasculature requires vascular imaging. Vascular imaging techniques of various types are used to identify vessels that should be avoided during SEEG implantation planning. The gold standard for cerebral vascular imaging is digital subtraction angiography (DSA) [32]. Li et al. studied the size of vessels, which is clinically significant for SEEG implantation planning. They found out that electrode conflicts with vessels 1- 1.5 mm in size did not result in radiologically detectable or clinically significant hemorrhages and suggested that vessels under 1-1.5 mm in diameter should be excluded from consideration during designing SEEG trajectory[33].

Nowadays, digital subtraction angiography (DSA), computed tomography angiography (CTA), or magnetic resonance angiography (MRA) all allow for high-resolution (diameter1.5 mm) vascular imaging[34,35]. The most widely utilized angiographic techniques are computed tomography (CT) angiography and digital subtraction angiography, although magnetic resonance angiography enables high-resolution vascular visualization without additional radiation dangers. In this study, based on CE-MRAV (Contrast-Enhanced Magnetic Resonance Angio-Venogram) all vessels that are greater than 1 mm in diameter will be imaged and visualized to ensure surgical safety. Therefore, all clinically relevant blood vessels can be visualized before SEEG implantation. Accurate co-registered 3D views of the vasculature and sulcal anatomy are critical for planning SEEG trajectories while avoiding blood vessels [36]. The SinoPlan system effectively applies the Angio Render technology, reconstructing individual 3D views of the sulcal and vasculature anatomy. These anatomical and vascular maps are possibly the main reason for the absence of intracerebral hemorrhages after implanting 634 SEEG electrodes. Stereotactic RF-TC was developed as a surgical treatment for focal epilepsy, primarily as an alternative to traditional surgery, between the 1970s and the 1990s. SEEG-guided RF-TC may be a significant therapeutic option when a large epileptic network (multifocal ictal onsets) is involved, which is inaccessible to the appropriate surgery. This contrasts with the situation of a limited volume epileptic zone accessible to a total or subtotal RF-TC lesion in a location where surgery is risky (such as periventricular heterotopia or insular ictal onset zone). In fact, the functional disruption of such a network could be caused by numerous lesions carried out in remote areas[37]. Even if a complete cure for epilepsy cannot be achieved in this manner, a significant improvement may take place, and patients occasionally develop drug sensitivity. These outcomes, meanwhile, are typically sporadic, probably because of the reconfiguration of the epileptic network. Repeating SEEG-guided RF-TC seems like a good possibility in this case, and the new intrusive information regarding potential modifications to the epileptic network may assist designate new, ideal targets to cause additional network disruption. Additionally, several procedural factors affect the efficiency and security of stereotactic RF-TC. includes RF delivery duration, the quantity of coagulation sites, the rate of power rise, the distance between the dipole contacts, and variations in the substrates that are coagulated.

Miller et al. researched the best way to spread out radiofrequency lesions over various SEEG electrodes[38]. The biggest lesions may be created when radiofrequency power was administered over a prolonged period at less than 3 W, according to both in vitro and in vivo study. The size of the lesion was also influenced by the linear separation of the electrodes, with the greatest lesions occurring when the linear gap was between 5 and 12 mm. Large clinical lesions with improved interictal and ictal activity were created utilizing these criteria. Both connections were encircled by confluent lesions that were formed. The greatest lesion, measuring 100.74 mm^2 (mean of 74. 1±11.3 mm^2), was produced with a power of 3 W at 8 mm of electrode spacing. To ensure the safety of RF-TC, it is crucial to establish the distance between the electrode and the blood vessel prior to performing stereotactic RF-TC. Examination of the radiofrequency lesions revealed that an electrode's distance from the blood vessel should not be less than 6 mm. The SinoPlan method efficiently employs Angio Render technology, reconstructing individual 3D representations of the sulcal and vascular anatomy[39]. This substantially simplifies determining the electrode's distance from the blood vessel following surgery.

This study demonstrated the utility of the SINO-robotic trajectory guidance system in the implantation of SEEG electrodes, with minimal error in entry and target points, no intervention complications, and a positive post-operative outcome after EZ ablation in many patients.

Limitations of the Study

In this study, the data was limited as it was a single-center study and with no controls. This article introduces the value of Angio render technology in clinical application, but it could not evaluate the hemorrhage incidence before electrode implantation and RFTC.

Conclusion

Our preliminary study on the adoption of the SINO robot-guided SEEG has demonstrated comparable mean operating time per lead, accuracy, and safety, compared to previously published robot-guided SEEG series. The SinoPlan system applies Angio Render technology, effectively achieving 3D visualization of vessel imaging and improving the safety of surgery. Ultimately, the SINO robot is a reliable and recommended guidance system.

Funding Statement:

This work was supported by Joint Funds for the Innovation of Science and Technology, Fujian province (Grant No 2018Y9059), Fujian Provincial Natural Science Foundation Program (Grant No 2021J01788.) and the Startup Fund for scientific research, Fujian Medical University (Grant No. 2021QH1048).

Competing Interests Statement:

The authors declare that they have no conflict of interest.

Contributor ship Statement:

RL has conceived and coordinated the study. SS and RJ have signed, performed, and analyzed the experiments, wrote the paper. YD and JZ, ZQ have carried out the data collection, data analysis. And SS has revised the paper. All authors reviewed the results and approved the final version of the manuscript.

Data Availability:

The datasets used and/or analyzed during the current study are available from the corresponding author on reasonable request.

Table1. Previously reported studies about stereotactic robots of electrode implantation

Vakharia et al. 2017 [5]; Martínez et al 2017[26]; Ollivier et al.,[40]; Ho et al., 2018[41]; Spyrantis et al., 2018 [12]; Iordanou et al., 2019[42]; Candela-Cantó et al., 2018 [8] Machetanz et al. 2020[43]; Machetanz et al. 2020[43]; Zhang et al.2021[9]; Yao et al. 2023[44]; Dedrickson et al. 2023[45]; Vasconcellos et al. 2023[25]; Zhao et al. 2023[46]; Gomes et al. 2023[24]; Gorbachuk et al. 2023[47]

Table2. Statistical analysis related to electrode implantation

Table3. Epilepsy outcomes after follow up in 58 patients who underwent SEEG

Figures

Fig. 1. Planning electrode trajectories directly in a three-dimensional view.

Fig. 2. Three-dimensional reconstructed images of four typical cases after electrode implantation. The epileptic lesion in Case (A) was in the right parietal occipital lobe, in Case (B), in the left frontal lobe, in Case (C), in a hypothalamic hamartoma, and in Case (D) in the left temporal lobe.

Fig. 3. Operation and SEEG electrode implantation (a) Patient registration image for recognition based on bone fiducials (b) Twist drill holes to the skull through the scalp under robotic arm guidance (c) Firmly screwed guidance anchor bolt into the hole (d) Puncturing the brain to open the electrode trajectory using a sterilized stylet (e) Mark

SEEG electrodes as target length (f) Rubber rings for SEEG electrodes were secured by polyurethane bolt caps.

Fig. 4. The target point localization errors were calculated for eachelectrode. The figure shows the case of hypothalamic hamartoma.

References

1. Rugg-Gunn F, Miserocchi A, McEvoy A. Epilepsy surgery. Pract Neurol 2020;20:4-14
2. Engel J, Jr. Evolution of concepts in epilepsy surgery. Epileptic Disord 2019;21:391-409
3. Cardinale F, Cossu M, Castana L, et al. Stereoelectroencephalography: surgical methodology, safety, and stereotactic application accuracy in 500 procedures. Neurosurgery 2013;72:353-366; discussion 366
4. Gholipour T, Koubeissi MZ, Shields DC. Stereotactic electroencephalography. Clin Neurol Neurosurg 2020;189:105640
5. Vakharia VN, Sparks R, O'Keeffe AG, et al. Accuracy of intracranial electrode placement for stereoencephalography: A systematic review and meta-analysis. Epilepsia 2017;58:921-932
6. van der Loo LE, Schijns O, Hoogland G, et al. Methodology, outcome, safety and in vivo accuracy in traditional frame-based stereoelectroencephalography. Acta Neurochir (Wien) 2017;159:1733-1746
7. Song S, Dai Y, Chen Z, Shi S. Accuracy and Feasibility Analysis of SEEG Electrode Implantation using the VarioGuide Frameless Navigation System in Patients with Drug-Resistant Epilepsy. J Neurol Surg A Cent Eur Neurosurg 2021;82:430-436
8. Candela-Cantó S, Aparicio J, López JM, et al. Frameless robot-assisted stereoelectroencephalography for refractory epilepsy in pediatric patients: accuracy, usefulness, and technical issues. Acta Neurochir (Wien) 2018;160:2489-2500
9. Zhang D, Cui X, Zheng J, et al. Neurosurgical robot-assistant stereoelectroencephalography system: Operability and accuracy. Brain Behav 2021;11:e2347
10. Cardinale F, Rizzi M, d'Orio P, et al. A new tool for touch-free patient registration for robot-assisted intracranial surgery: application accuracy from a phantom study and a retrospective surgical series. Neurosurg Focus 2017;42:E8
11. Brandmeir NJ, Savaliya S, Rohatgi P, Sather M. The comparative accuracy of the ROSA stereotactic robot across a wide range of clinical applications and registration techniques. J Robot Surg 2018;12:157-163
12. Spyrantis A, Cattani A, Strzelczyk A, et al. Robot-guided stereoelectroencephalography without a computed tomography scan for referencing: Analysis of accuracy. Int J Med Robot 2018;14
13. Lu C, Chen S, An Y, et al. How can the accuracy of SEEG be increased?-an analysis of the accuracy of multilobe-spanning SEEG electrodes based on a frameless stereotactic robot-assisted system. Ann Palliat Med 2021;10:3699-3705
14. Abel TJ, Varela Osorio R, Amorim-Leite R, et al. Frameless robot-assisted stereoelectroencephalography in children: technical aspects and comparison with Talairach frame technique. J Neurosurg Pediatr 2018;22:37-46
15. Liu W, Guo H, Du X, et al. Cortical vessel imaging and visualization for image guided depth electrode insertion. Comput Med Imaging Graph 2013;37:123-130
16. Kwan P, Arzimanoglou A, Berg AT, et al. Definition of drug resistant epilepsy: consensus proposal by the ad hoc Task Force of the ILAE Commission on Therapeutic Strategies. Epilepsia 2010;51:1069-1077

17. Isnard J, Taussig D, Bartolomei F, et al. French guidelines on stereoelectroencephalography (SEEG). Neurophysiol Clin 2018;48:5-13
18. Mascia A, Casciato S, De Risi M, et al. Bilateral epileptogenesis in temporal lobe epilepsy due to unilateral hippocampal sclerosis: A case series. Clin Neurol Neurosurg 2021;208:106868
19. Liu Q, Mao Z, Wang J, et al. The accuracy of a novel self-tapping bone fiducial marker for frameless robot-assisted stereo-electro-encephalography implantation and registration techniques. Int J Med Robot 2023;19:e2479
20. Moles A, Guénot M, Rheims S, et al. SEEG-guided radiofrequency coagulation (SEEG-guided RF-TC) versus anterior temporal lobectomy (ATL) in temporal lobe epilepsy. J Neurol 2018;265:1998-2004
21. Lee CY, Li HT, Wu T, et al. Efficacy of limited hippocampal radiofrequency thermocoagulation for mesial temporal lobe epilepsy. J Neurosurg 2018;131:781-789
22. Guénot M, Isnard J, Ryvlin P, et al. SEEG-guided RF thermocoagulation of epileptic foci: feasibility, safety, and preliminary results. Epilepsia 2004;45:1368-1374
23. Tabak J. Geometry: the language of space and form: Infobase Publishing; 2014
24. Gomes FC, Larcipretti ALL, Nager G, et al. Robot-assisted vs. manually guided stereoelectroencephalography for refractory epilepsy: a systematic review and meta-analysis. Neurosurg Rev 2023;46:102
25. Vasconcellos FDNAA, Timoteo %A Fiedler, Augusto Müller %A Fountain, Hayes %A Piedade, Guilherme Santos %A Monaco, Bernardo A %A Jagid, Jonathan %A Cordeiro, Joacir G. Robotic-Assisted Stereoelectroencephalography: A Systematic Review and Meta-Analysis of Safety, Outcomes, and Precision in Refractory Epilepsy Patients. Cureus 2023
26. González-Martínez J, Bulacio J, Thompson S, et al. Technique, Results, and Complications Related to Robot-Assisted Stereoelectroencephalography. Neurosurgery 2016;78:169-180
27. Cardinale F, Casaceli G, Raneri F, Miller J, Lo Russo G. Implantation of Stereoelectroencephalography Electrodes: A Systematic Review. J Clin Neurophysiol 2016;33:490-502
28. Guenot M, Isnard J, Ryvlin P, et al. Neurophysiological monitoring for epilepsy surgery: the Talairach SEEG method. StereoElectroEncephaloGraphy. Indications, results, complications and therapeutic applications in a series of 100 consecutive cases. Stereotact Funct Neurosurg 2001;77:29-32
29. Derrey S, Lebas A, Parain D, et al. Delayed intracranial hematoma following stereoelectroencephalography for intractable epilepsy: case report. J Neurosurg Pediatr 2012;10:525-528
30. Serletis D, Bulacio J, Bingaman W, Najm I, González-Martínez J. The stereotactic approach for mapping epileptic networks: a prospective study of 200 patients. J Neurosurg 2014;121:1239-1246
31. Mullin JP, Shriver M, Alomar S, et al. Is SEEG safe? A systematic review and meta-analysis of stereo-electroencephalography-related complications. Epilepsia 2016;57:386-401
32. Jung SC, Kang DW, Turan TN. Vessel and Vessel Wall Imaging. Front Neurol Neurosci 2016;40:109-123
33. Li K, Vakharia VN, Sparks R, et al. Stereoelectroencephalography electrode placement: Detection of blood vessel conflicts. Epilepsia 2019;60:1942-1948
34. Feng AY, Ho AL, Kim LH, et al. Utilization of Novel High-Resolution, MRI-Based Vascular Imaging Modality for Preoperative Stereoelectroencephalography Planning in Children: A Technical Note. Stereotact Funct Neurosurg 2020;98:1-7
35. Vakharia VN, Sparks R, Vos SB, et al. The Effect of Vascular Segmentation Methods on Stereotactic Trajectory Planning for Drug-Resistant Focal Epilepsy: A Retrospective Cohort Study. World Neurosurg X 2019;4:100057
36. Cardinale F, Pero G, Quilici L, et al. Cerebral Angiography for Multimodal Surgical Planning in Epilepsy Surgery: Description of a New Three-Dimensional Technique and Literature Review. World Neurosurg 2015;84:358-367
37. Bourdillon P, Devaux B, Job-Chapron AS, Isnard J. SEEG-guided radiofrequency thermocoagulation. Neurophysiol Clin 2018;48:59-64
38. Staudt MD, Maturu S, Miller JP. Radiofrequency Energy and Electrode Proximity Influences Stereoelectroencephalography-Guided Radiofrequency

Thermocoagulation Lesion Size: An In Vitro Study with Clinical Correlation. Oper Neurosurg (Hagerstown) 2018;15:461-469
39. Du X, Ding H, Zhou W, Zhang G, Wang G. Cerebrovascular segmentation and planning of depth electrode insertion for epilepsy surgery. Int J Comput Assist Radiol Surg 2013;8:905-916
40. Ollivier I, Behr C, Cebula H, et al. Efficacy and safety in frameless robot-assisted stereo-electroencephalography (SEEG) for drug-resistant epilepsy. Neurochirurgie 2017;63:286-290
41. Ho AL, Muftuoglu Y, Pendharkar AV, et al. Robot-guided pediatric stereoelectroencephalography: single-institution experience. J Neurosurg Pediatr 2018;22:1-8
42. Iordanou JC, Camara D, Ghatan S, Panov F. Approach Angle Affects Accuracy in Robotic Stereoelectroencephalography Lead Placement. World Neurosurg 2019;128:e322-e328
43. Machetanz K, Grimm F, Wuttke TV, et al. Frame-based and robot-assisted insular stereo-electroencephalography via an anterior or posterior oblique approach. J Neurosurg 2021;135:1477-1486
44. Yao Y, Hu W, Zhang C, et al. A comparison between robot-guided and stereotactic frame-based stereoelectroencephalography (SEEG) electrode implantation for drug-resistant epilepsy. J Robot Surg 2023;17:1013-1020
45. Dedrickson T, Davidar AD, Azad TD, Theodore N, Anderson WS. Use of the Globus ExcelsiusGPS System for Robotic Stereoelectroencephalography: An Initial Experience. World Neurosurg 2023;175:e686-e692
46. Li P, Zhou Y, Zhang Q, et al. Frameless robot-assisted stereoelectroencephalography-guided radiofrequency: methodology, results, complications and stereotactic application accuracy in pediatric hypothalamic hamartomas. Front Neurol 2023;14:1259171
47. Gorbachuk M, Machetanz K, Weinbrenner E, et al. Robot-assisted stereoencephalography vs subdural electrodes in the evaluation of temporal lobe epilepsy. Epilepsia Open 2023;8:888-897

Table2. Statistical analysis related to electrode implantation

No. of patients	58
Bilateral implantation	6
No. of implanted electrodes	634
Mean no. of electrodes/patient	10.92 (range: 5– 18)
Mean operating time per electrode(min)	6. 18±1.80 (range: 3.02– 14.61)
Mean errors	
Entry point error (mm)	0.94 ± 0.23 (range: 0.39– 1.63)
Target point error (mm)	1.49 ± 0.37 (range: 0.80–2.78)
Target point location	
Frontal	30.44%(193/634)
Temporal	35.48%(225/634)
Parietal	12.30%(78/634)
Occipital	9.78%(62/634)
Insula	5.85%(37/634)
Hypothalamic Hamartoma	6.15%(39/634)
Mean depth （mm）	
Mean depth of all electrodes	56.96± 3.62(range:27.23–124.85)
Mean depth of electrodes which target to Frontal	47.49± 0.65(range:41.6–54.91)
Mean depth of electrodes which target to Temporal	66.70± 1.92(range:46.13–124.85)
Mean depth of electrodes which target to Parietal	41.27± 2.47(range:32.48–61.26)
Mean depth of electrodes which target to Occipital	50.41± 2.96(range:27.23–63.28)
Mean depth of electrodes which target to Insula	54.37±3.33(range:47.79–72.13)
Mean depth of electrodes which target to Hypothalamic Hamartoma	91.91± 0.93(range:84.06–108.61)

*Values expressed as the mean±SD

Table3. Epilepsy outcomes after follow up in 58 patients who underwent SEEG

SEEG& Epilepsy Outcomes	Value
Seizure capture	100%
Duration of monitoring（days）	14.58±4.27
Length of stay(days)	15.91±2.83
Epileptogenic zone localization	100%
Follow-up(mos)	14.37±1.57
Resection	17
Engel class	
I	82.35%（14/17）
II	17.65%（3/17）
III	0
IV	0
Histology	
Hippocampus sclerosis	5
FCD	6
TSC	3
Gliosis	3
RF-TC	41
Engel class	
I	80.48%（33/41）
II	14.63 %（6/41）
III	4.89%（2/41）

IV	0

*Values expressed as the mean±SD；TSC, Tuberous Sclerosis Complex;FCD, focal cortical dysplasia

Table1. Previously reported studies about stereotactic robots of electrode implantation

Article	Method	Patients	Electrodes (Total)	Electrodes/ case	Mean time per electrode (min)	Entry point accuracy(mm)	Target point accuracy (mm)
Vakharia et al. 2017[5]	Robotic trajectory guidance system	/		/	/	1.17 (0.80–1.53 95%CI)	1.71 mm (interquartile range, 1.20-2.30 mm).
Martínez et al 2017[26]	ROSA robotic	101	1245	12.5	10.4	1.2 mm (interquartile range, 0.78- 1.83 mm)	1.7 mm (interquartile range, 1.20-2.30 mm).
Ollivier et al., 2017[40]	ROSA robotic	66	857	12.98	9.01	1. 1 (0.15–2.48)	2.09(1.06–3.72)
Ho et al., 2018[41]	ROSA robotic	7	222	11.1	10.98	1.75±0.94 (range of 0.91–3.62)	3.39±1.078 (range of 0.9–4.02)
Spyrantis et al., 2018[12]	ROSA robotic	5	40	8	9.38	2.96±0.24	2.53±0.24
Iordanou et al., 2019 [42]	ROSA robotic	25	Oblique 109	/	/	1.76 SD 1.62	/
			Orthogonal 210	/	/	1.32 SD 1.19	/

Candela-Cantó et al.2018 [8]	Robotic arm Neuromate (Renishaw®)	14	164	/	/	1.57 (range of 1–2.25)	1.77 (range of 1.2–2.6)
Machetanz et al. 2020[43]	frame (Radionics Brown-Roberts-Wells,)	12	91	7.58	15.1 ± 1.9	1.5 ± 0.6	1.5 ± 0.8
	ROSA	15	129	8.6	9.1 ± 1.7	0.7 ± 0.5	1.6 ± 0.8
Zhang et al.2021[9]	SINO Robotic	16	162	10. 13 ± 2.70	10. 13 ± 2.70	1.56 (IQR0.00,2.24)	1.56 (IQR0.00,2.24)
Yao et al. 2023[44]	SINO Robotic	87	777	8.9 ± 2.2	7.9 ± 1.3	1.48 ± 1.46	1.61 ± 1.3
	CRW stereotactic frame	60	464	7.9 ± 2.5	13.5 ± 3.1	1.59 ± 0.9	1.64 ± 1.3
Dedrickson et al. 2023[45]	Globus ExcelsiusGPS robot	5	59	11.8 ± 3.7	/	1.6 ± 1.2 mm	/
Vasconcellos et al. 2023[25]	Overall	811	8184	10.06	15.1	1.48(rang 0-8.37)	2.13 (rang 0-7.3)
	ROSA	411	4848	11.8	11.45	1.49 (rang0.3-6.38)	2.5 (rang 0-9.02)
	Neuromate	202	1585	7.8	36.6	1.66 (rang0-8.37)	2.09 (rang 0-7.33)
	Sinovation	140	1330	9.5	9.9	1.39 (rang /)	1.64(rang 0.33-3.61)
	ISys1	58	421	7.25	15.7	1.23 (rang 0.1-3.4)	1.61 (rang 0.3-6.7)

Zhao et al. 2023[46]	SINO Robotic	28	161	5.75	/	0.87 mm(interquartile range, 0.50–1.41 mm)	2.74 mm (interquartile range, 2.01–3.63 mm)
Gomes et al. 2023[24]	Robotic-assisted	232	/	8.5 - 15.6	MD-3.35min;95% CI-3.68,-3.03;p<0.00001	MD 0.04 mm; 95% CI 0.21,-0.29; p = 0.76	MD-0.57 mm; 95% CI-1.08; -0.06; p = 0.03
	Traditional hand-guided	196	/	4.5 - 12.56			
Gorbachuk et al. 2023[47]	SINO Robotic	20	185	9.25	7.9 ± 2.3	/	/
Present study	SINO Robotic	58	634	10.92(range 5-18)	6.18 ± 1.80 min (range:3.02– 14.61 min)	0.94 ± 0.23mm(range: 0.39– 1.63）	1.49 ± 0.37 mm (range: 0.80–2.78 mm)

Complications
Not specified
4 patients (4%)2 subdural hematomas and 2 intraparenchymal hematomas
1 patient symptomatic brain hematomas,8 patients asymptomatic postoperative bleeding
Nil
Nil
Not specified

1 patient meningitis without demonstrated germ ;1 patient right frontal hematoma

Intracranial hemorrhage 3 (5.0%)

1 patient subdural hematoma

Not specified

Intracranial hemorrhage 6 (6.7%)

Intracranial hemorrhage 6 (6.7%)

no complications

/

4/152electrodes bleeding

intracranial hemorrhage
9/145 (6.2%)

intracranial hemorrhage
8/139 (5.7%)

2/20 (10%)Patients
Bleeding ;2/185
(1%)Electrodes Bleeding

2 patient asymptomatic
brain hematomas

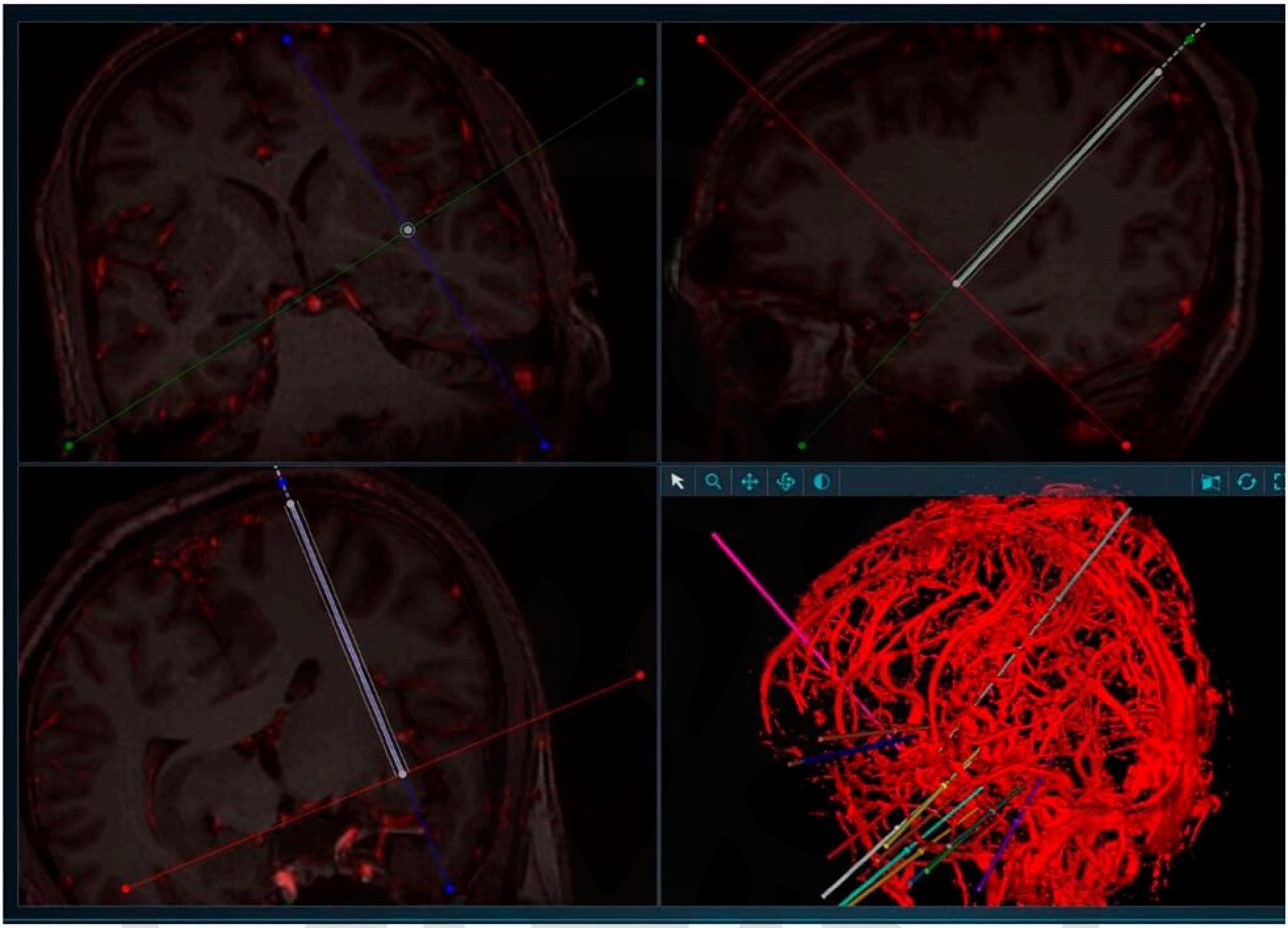

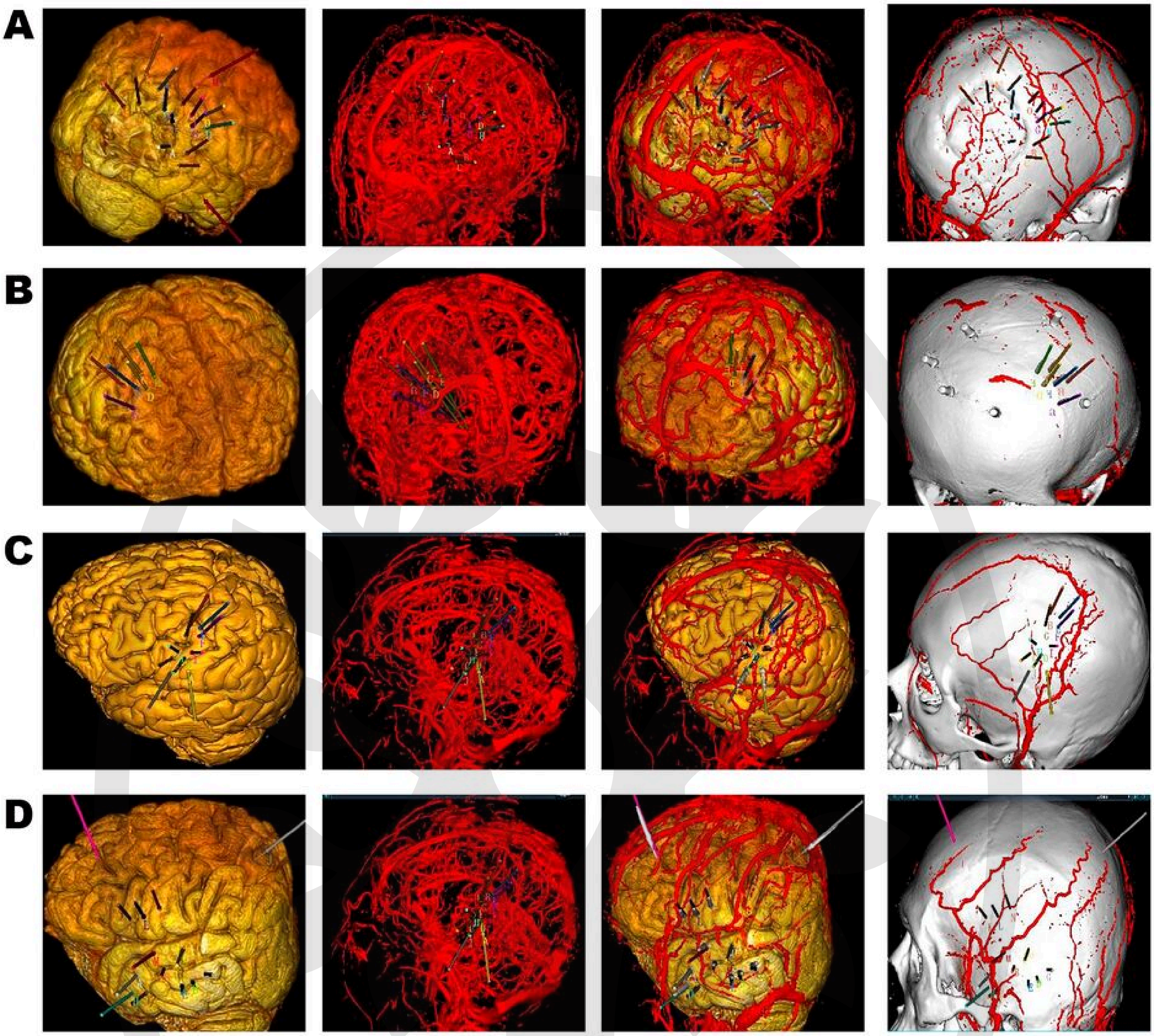
A
B
C
D

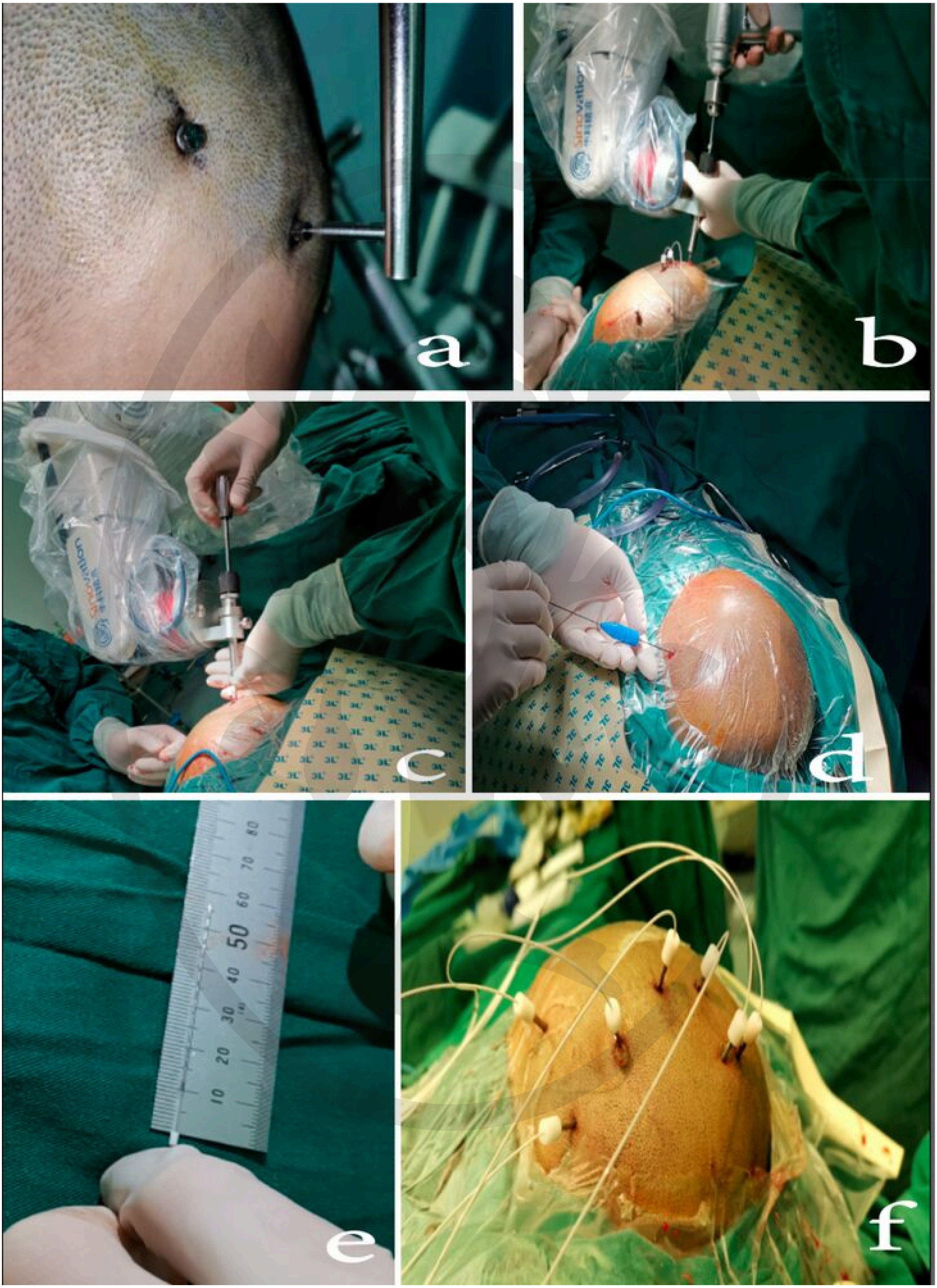
a
b
c
d
e
f
Sinovation
10
20
30
40
50
60
70
80

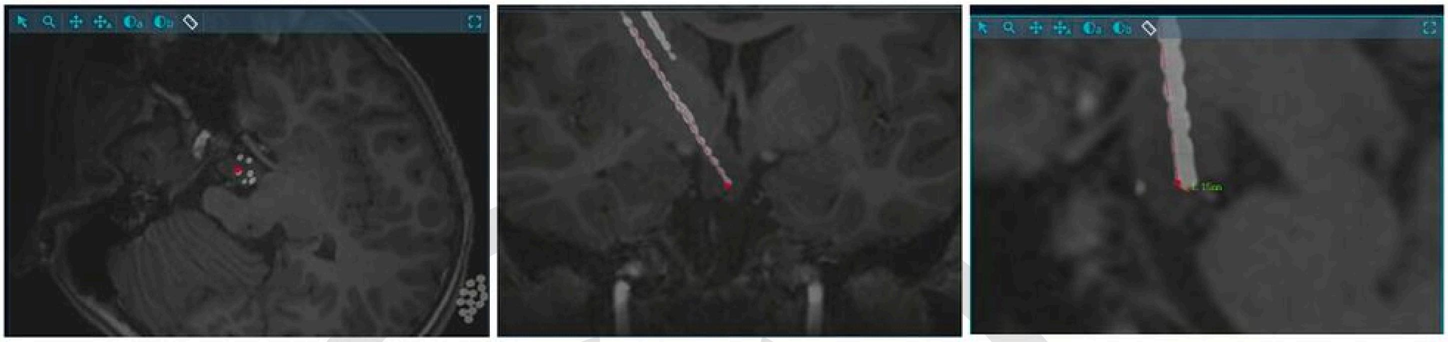
L 15mm